Reppel, Julie-Ann; Alwahabi, Zeyad T..
Orthogonal planar laser polarization spectroscopy, *Applied Optics*, 2002; 41 (21):4267-4272.

Orthogonal planar laser polarization spectroscopy

Julie Reppel and Zeyad T. Alwahabi

Planar laser polarization spectroscopy has recently been used to image the hydroxyl radical in combustion for small intersection angles of pump and probe beams. We report an experimental configuration that allows planar laser polarization imaging for perpendicular intersection of pump and probe beams. We demonstrate what to our knowledge is the first planar laser polarization spectroscopy imaging at a 90° intersection of pump and probe beams for both linearly and circularly polarized pump beams. © 2002 Optical Society of America

OCIS codes: 120.0120, 120.1740.

1. Introduction

Polarization spectroscopy is based on detection of the induced polarization change in a weak probe beam that is due to the passage of a strong pump laser beam through an optically thin medium. A strong linearly or circularly polarized pump beam is used to create population anisotropy of Zeeman sublevels. A weak linearly polarized probe beam that crosses the pump beam path experiences linear birefringence and dichroism that are due to the Zeeman population anisotropy if the probe polarization direction contains components that are parallel and perpendicular to the pump beam polarization. The signal strength is maximized if the probe beam polarization is equally divided between parallel and perpendicular components. For a circularly polarized pump beam, the linearly polarized probe beam undergoes circular dichroism and birefringence. The weak polarization signal is detected by placement of crossed polarizers in the probe beam path that enclose the pump–probe beam intersection volume.

Conventionally, polarization spectroscopy is implemented in a counterpropagating, Doppler-free[1] pump and probe beam geometry to maximize signal strength. However, polarization spectroscopy imaging requires a finite beam intersection angle.

J. Reppel and Z. T. Alwahabi (zalwahab@chemeng.adelaide.edu.au) are with the Department of Chemical Engineering, Adelaide University, Adelaide, S.A. 5005, Australia. J. Reppel is also with the Department of Mechanical Engineering.

Received 8 June 2001; revised manuscript received 3 March 2002.

0003-6935/02/214267-06$15.00/0

Polarization spectroscopy imaging of the hydroxyl radical in a premixed CH_4/O_2 flame for pump–probe beam intersection angles of 15° and 30° has been demonstrated by Nyholm *et al.*[2] The linearly polarized probe beam intersected a horizontally polarized pump laser sheet, and the probe beam was polarized at 45° to the vertical. The OH distribution within the elliptical interaction region was imaged on the circular cross section of the pump beam. The signal strength was shown experimentally to follow a $\cot^2(\theta)$ dependence on the intersection angle of pump and probe beams θ. A $\cot^2(\theta)$ dependence of polarization spectroscopy signal strength in the weak saturation regime was previously noted by Zizak *et al.*[3] for the case of a circularly polarized pump beam. The Zizak *et al.* experiment was limited to pump–probe beam intersection angles of less than 30° owing to weak signal strength. Zizak *et al.*[3] and Nyholm *et al.*[2] explained the $\cot^2(\theta)$ dependence in terms of the combined effects of the change in the interaction volume between pump and probe beams and the projection of the pump beam polarization on that of the probe beam.

The reported $\cot^2(\theta)$ falloff in signal strength with increasing intersection angle leads to a zero signal strength for a pump–probe beam intersection angle of 45°. In imaging applications, the decreased signal strength must be matched against increased horizontal resolution of the imaged elliptical cross section. Here we report an experimental configuration based on recent theoretical results[4] that leads to a nonzero signal at a 90° pump–probe intersection angle. The configuration can relax the small intersection angle requirement for polarization spectroscopy imaging.

2. Theory

For perfectly crossed probe beam polarizers, the polarization spectroscopy signal is given by[5]

$$I = I_{\text{probe}}\left[\xi + \frac{1}{16}(\Delta\alpha L)^2 L(x)\right], \tag{1}$$

where I is the detected intensity, I_{probe} is the input probe beam intensity, ξ represents the extinction ratio of the probe beam polarizers, $\Delta\alpha$ is the induced dichroism, L is the interaction distance of pump and probe beams measured along the probe beam path, $L(x)$ represents the line-shape function, recently calculated by Reichardt and Lucht[6] to be Lorentzian cubed in the low saturation regime, and x is the detuning from resonance.

The geometric dependence of the polarization spectroscopy signal strength lies in the terms $\Delta\alpha$ and L. The pump–probe interaction length L is given by

$$L = W/\sin(\theta), \tag{2}$$

where W is the width of the pump sheet, which contributes a $\csc^2(\theta)$ factor to the overall signal dependence.

The induced dichroism $\Delta\alpha$ is related to the induced birefringence Δn by the Kramers–Kronig relations. Reppel and Alwahabi[4] derived an expression for the geometric dependence of the induced linear birefringence for the case of a linearly polarized pump beam by proposing that the optical properties of the pumped region be analogous to the birefringent properties of a uniaxial crystal. An equivalent expression for the induced circular birefringence in the case of a circularly polarized pump beam was derived by analogy with the optical properties of an optically active uniaxial crystal.

The ordinary refractive index, n_o, is independent of the direction of propagation. In a uniaxial crystal, however, the effective extraordinary refractive index, $n(\theta)_e$, is a function of the angle of propagation from optic axis θ, The magnitude of the effective birefringence, $|\Delta n(\theta)| = |n(\theta)_e - n_o|$, oscillates between a maximum value, $\Delta n_{\max} = |n_e - n_o|$, for propagation normal to the optic axis and zero for propagation along the optic axis.

For polarization spectroscopy, the induced optic axis can be defined as the polarization direction of the pump beam. Assuming that the induced birefringence is small, Reppel and Alwahabi[4] showed that the linear birefringence induced by a linearly polarized pump beam is

$$n(\theta)_e - n_o = \sin^2(\varphi)(n_e - n_o), \tag{3}$$

where φ is the angle between the direction of propagation of the probe beam and the induced optic axis (corresponding to the polarization direction of the pump beam). It can easily be seen that, for pump and probe beams intersecting in the horizontal plane at angle θ, a horizontally polarized pump beam leads to a $\cos^2(\theta)$ dependence of the induced birefringence. The resultant polarization spectroscopy signal strength I, when the pump beam is horizontally polarized, is

$$I = I_{\text{probe}}\left\{\xi + \frac{1}{16}\left[\frac{\cos^2(\theta)}{\sin^2(\theta)}\right]\Delta\alpha_{\max(\text{linear})}{}^2 L^2\, L(x)\right\}, \tag{4}$$

which follows the $\cot^2(\theta)$ dependence reported by Nyholm *et al.*[2] The term $\Delta\alpha_{\max(\text{linear})}$ is the maximum induced dichroism for collinear pump and probe beams. This dichroism was evaluated by Teets *et al.*[5] by means of summation, over the Zeeman states of the lower level of the probe beam transition, of functions of the Clebsch–Gordon coefficients. The dichroism is related to the maximum induced birefringence $\Delta n_{\max(\text{linear})}$ by the Kramers–Kronig relations.

A vertically polarized pump beam pump, however, induces a linear birefringence that is independent of the intersection angle of pump and probe beams. The polarization spectroscopy signal strength for a vertically polarized pump beam then follows a $\csc^2(\theta)$ dependence on pump–probe beam intersection angle

$$I = I_{\text{probe}}\left\{\xi + \frac{1}{16}\left[\frac{1}{\sin^2(\theta)}\right]\Delta\alpha_{\max(\text{linear})}{}^2 L^2\, L(x)\right\}. \tag{5}$$

Note that Eqs. (4) and (5) assume that the probe beam is polarized at 45° to the pump beam polarization axis.

Reppel and Alwahabi[4] derived a general expression for the linear dichroism induced by a linearly polarized pump beam by considering pump and probe beams intersecting at angle θ in a horizontal plane. The pump beam was polarized at angle κ, and the probe beam was polarized at angle γ to the vertical. In each case, the vertical axis and the direction of propagation of the beam represent the X and Z axes, respectively, of a right-handed system to define the positive direction of rotation of angles κ and γ. The polarization spectroscopy signal strength I for a linearly polarized pump beam is written as

$$I = I_{\text{probe}}\left[\xi + \frac{1}{16}F(\gamma, \kappa, \theta)_{\text{lin}}\,\Delta\alpha_{\max(\text{linear})}{}^2 L^2\, L(x)\right], \tag{6}$$

where the geometric dependence is contained in the factor $F(\gamma, \kappa, \theta)_{\text{lin}}$:

$$F(\gamma, \kappa, \theta)_{\text{lin}} = \frac{1}{\sin^2(\theta)}\,\frac{\{\sin(2\gamma)[\cos^2(\kappa) - \sin^2(\kappa)\cos^2(\theta)] - \cos(2\gamma)\sin(2\kappa)\cos(\theta)\}^2}{[1 - \sin^2(\kappa)\sin^2(\theta)]}. \tag{7}$$

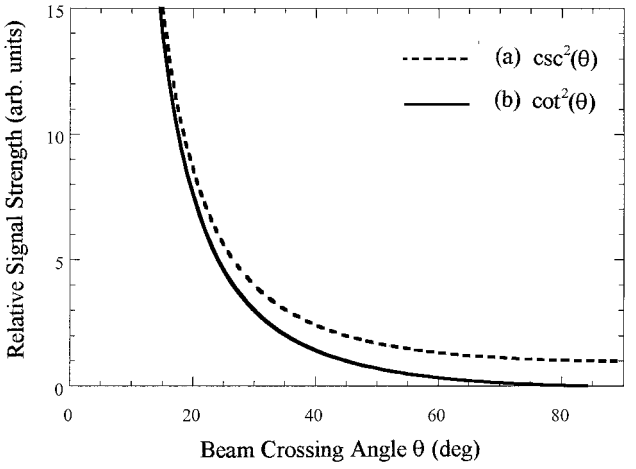

Fig. 1. Dependence of polarization spectroscopy signal strength on pump–probe beam intersection angle θ for a pump beam polarized (a) in the plane of intersection and (b) normal to the plane of intersection.

For copropagating and counterpropagating pump beams, Eq. (7) reduces to

$$F(\gamma, \kappa, 0)_{\text{lin}} = \frac{\sin^2[2(\gamma - \kappa)]}{\sin^2(\theta)}, \tag{8}$$

$$F(\gamma, \kappa, \pi)_{\text{lin}} = \frac{\sin^2[2(\gamma + \kappa)]}{\sin^2(\theta)}, \tag{9}$$

respectively. For a horizontally polarized pump beam and a probe beam polarized at 45° to the vertical, Eq. (7) reduces to the $\cot^2(\theta)$ dependence noted in Eq. (4). Similarly, for a vertically polarized pump beam and a probe beam polarized at 45° to the vertical, the equation reduces to the $\csc^2(\theta)$ dependence of Eq. (5).

These two functions are plotted in Fig. 1. The $\cot^2(\theta)$ function drops to zero signal for a 90° intersection of pump and probe beams, whereas the $\csc^2(\theta)$ function exhibits nonzero signal strength for a 90° pump–probe intersection. The $\csc^2(\theta)$ signal decreases rapidly with an increased intersection angle. However, for the purpose of imaging, pump–probe intersection at 90° is desirable. The gain in resolution at the orthogonal intersection of pump and probe beams is optimized against the decreased signal strength at the large pump–probe beam intersection angles. If we assume that a minimum intersection angle of 10° is required for effective imaging, the ratio of signal strengths for imaging at 10° and 90° is 33:1. However, the ratio of signal strengths drops by only a factor of 4 for polarization spectroscopy imaging between the pump–probe intersection angles of 30° and 90°.

The Reppel and Alwahabi[4] expressions for geometric dependence, $F(\gamma, \theta)_{\text{lin}}$, of the polarization spectroscopy signal strength for a circularly polarized pump beam are based on an approximate expression for the induced birefringence between two polarization modes of propagation for the optically active uniaxial crystal, α and β:

$$n(\theta)_\alpha - n(\theta)_\beta = n_o\left[\sin^4(\theta)\left(\frac{\Delta + \sigma^2}{2}\right)^2 + \cos^2(\theta)\sigma^2\right]^{1/2}. \tag{10}$$

The terms $\Delta/2$ and σ are identified as the maximum induced linear dichroism and the maximum induced circular dichroism, respectively, and were calculated by Teets *et al.*[5]

The expressions for geometric dependence of the polarization spectroscopy signal strength are based on two regions of approximation. For probe beam propagation close to the optic axis, defined as the polarization axis of the circularly polarized pump beam, the induced birefringence is approximated by

$$n(\theta)_\alpha - n(\theta)_\beta = \cos(\theta)\sigma\, n_o. \tag{11}$$

For probe beam propagation near normal to the optic axis,

$$n(\theta)_\alpha - n(\theta)_\beta = \sin^2(\theta)\,\frac{(\Delta + \sigma^2)}{2}\, n_o. \tag{12}$$

The geometric dependences of the signal strength for these two regions of interest are

$$F(\gamma, \theta)_{\text{circ}(\theta\sim 0)} = \frac{1}{\sin^2(\theta)\cos^2(\theta)} \times \left\{ \begin{array}{l} [\cos^2(\gamma)\sin^4(\theta)\Delta + \cos^2(\theta)\sigma]^2 \\ + \dfrac{1}{4}[\cos(\theta)\sin^2(\theta)\sin(2\gamma)(\Delta - \sigma^2)]^2 \end{array} \right\} \tag{13}$$

for $\cos^2(\theta) \ll \sigma^2, \Delta$, and

$$F(\gamma, \theta)_{\text{circ}[\theta\sim(\pi/2)]} = \sin^2(2\gamma)\sin^2(\theta)\left(\frac{\Delta + \sigma^2}{2}\right)^2 \tag{14}$$

for $\cos^2(\theta) \gg \sigma^2, \Delta$. Note that, for Eqs. (13) and (14), the maximum induced linear and circular dichroisms have been included in the geometric dependence of the polarization spectroscopy signal strength.

The polarization axis of the circularly polarized pump beam lies parallel to the direction of propagation. For pump and probe beams that intersect at angle θ in the horizontal plane and a probe beam polarized in the horizontal plane, Eq. (13) reduces to

$$F\left(\frac{\pi}{2}, \theta\right)_{\text{circ}(\theta\sim 0)} = \cot^2(\theta)\sigma^2, \tag{15}$$

indicating a rapid falloff in signal strength with an increased angle of the pump–probe intersection. However, for normal incidence of pump and probe beams and an unspecified probe beam polarization direction, Eq. (14) can be rewritten as

$$F\left(\gamma, \frac{\pi}{2}\right)_{\text{circ}[\theta\sim(\pi/2)]} = \sin^2(2\gamma)\left(\frac{\Delta + \sigma^2}{2}\right)^2, \tag{16}$$

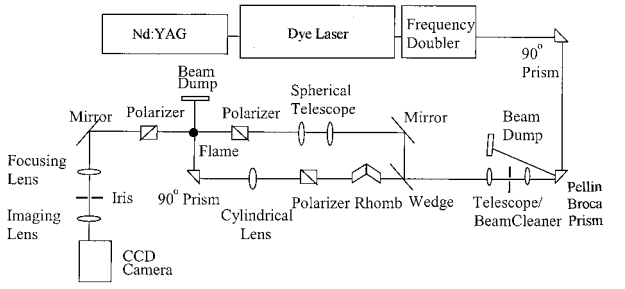

Fig. 2. Schematic diagram of the orthogonal intersection polarization spectroscopy experiment.

indicating that zero signal strength can be obtained for probe beam polarizations normal to or lying in the plane of incidence of the pump and probe beams.

3. Experiment

Figure 2 shows the experimental configuration used to image the OH radical in a premixed CH_4/O_2 flame for a 90° intersection of pump and probe beams for a linearly polarized pump beam. The pump beam is vertically polarized and the probe beam is polarized at 45° to the pump polarization. A Nd:YAG laser (Continuum Surelite) pumps a tunable dye laser (Lambda Physik Scanmate) with Rhodamine 101 dye. The output from the dye laser, 619.5 nm (0.15-cm^{-1} linewidth), is directed to the Scanmate UV doubling unit to double its frequency and separate the doubled UV radiation from the unconverted visible component. The estimated pulse width of the second harmonic is ~5 ns. The UV component emerges horizontally polarized from the doubling system. A telescope–spatial filter (magnification 4:1) expands and cleans the beam cross section. The front face reflection from a fused-silica wedge is used as the weak probe beam. The remainder of the pump beam is redirected by a fused-silica right-angle prism to pass through a half-wave Fresnel rhomb that rotates the plane of polarization through 90°. The pump beam passes through a vertically aligned Glan–Taylor polarizer. A cylindrical telescope produces the thin sheet that passes through the flame and intersects the weak probe beam, which was expanded by a spherical telescope (magnification 2:1) as it passed through the flame. The probe beam passes through a pair of crossed Glan–Taylor polarizers (extinction ratio estimated as $\sim 5 \times 10^{-6}$) enclosing the premixed flame. The pump and probe beams intersect at 90°. After it passes through the analyzer, the probe beam is redirected by an aluminum mirror and passes through two spherical lenses and an iris to be detected by an intensified CCD-576E (576 × 384 pixel array) Princeton Instruments camera gated at 20 ns. For a circularly polarized pump beam, the half-wave Fresnel rhomb placed in front of the pump beam polarizer is removed and a quarter-wave Fresnel rhomb is placed in the pump beam path behind the pump beam polarizer. The probe beam in both cases is polarized at 45° to the plane of intersection of pump and probe beams.

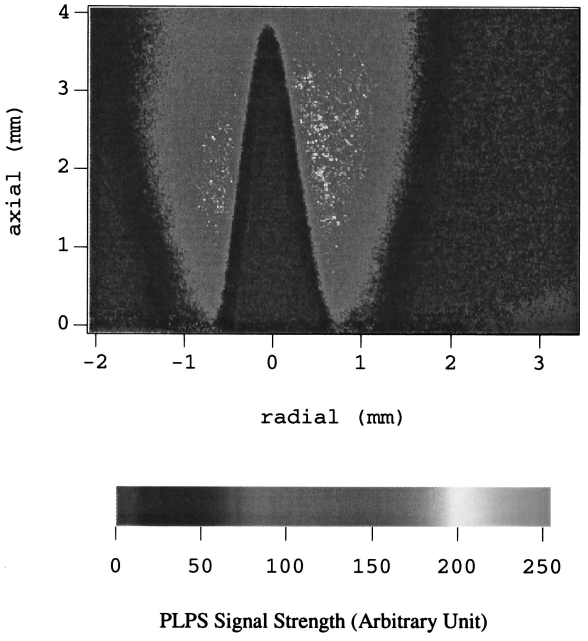

Fig. 3. Average OH [$A\,^2\Sigma$–$X\,^2\Pi$(0–0) $Q_2(8)$ transition] orthogonal PLPS signal in a laminar premixed CH_4/O_2 flame produced by a 1-mm jet exit diameter burner (Re ~ 3050). The pump beam is vertically polarized and the probe beam is polarized at 45° from the vertical.

The UV pump and probe beam pulse energies were estimated as 4 and 0.16 mJ, respectively, before they passed through the system optics. The pump sheet height was 25 mm and the sheet thickness was <0.6 mm. The probe beam was expanded to an area of 35 mm × 10 mm.

Figures 3 and 4 demonstrate orthogonal planar laser polarization spectroscopy (PLPS) imaging of the OH radical in a premixed CH_4/O_2 flame for a 90°

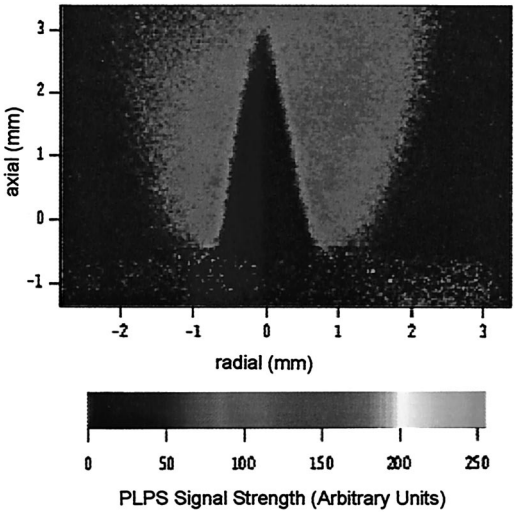

Fig. 4. Average OH [$A\,^2\Sigma$–$X\,^2\Pi$(0–0) $Q_2(8)$ transition] orthogonal PLPS signal in a laminar premixed CH_4/O_2 flame produced by a 1-mm jet exit diameter burner (Re ~ 3050). The pump beam is circularly polarized and the probe beam is polarized at 45° from the vertical.

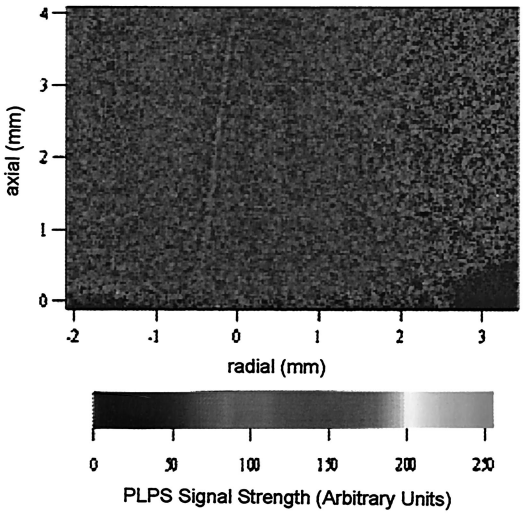

Fig. 5. Average OH [$A\ ^2\Sigma$–$X\ ^2\Pi$(0–0) $Q_2(8)$ transition] orthogonal PLPS signal in a laminar premixed CH_4/O_2 flame produced by a 1-mm jet exit diameter burner (Re ~ 3050). The pump beam is horizontally polarized and the probe beam is polarized at 45° from the vertical. The lack of signal supports the $\cot^2(\theta)$ dependence of signal strength for this polarization configuration noted by Nyholm *et al.*[2]

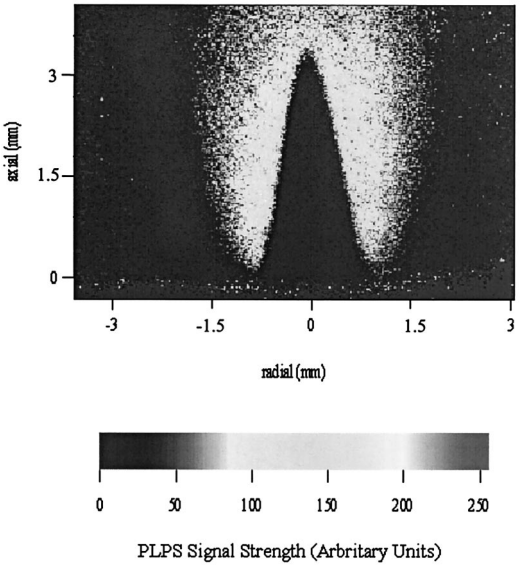

Fig. 6. Instantaneous OH [$A\ ^2\Sigma$–$X\ ^2\Pi$(0–0) $Q_2(8)$ transition] orthogonal PLPS signal for the laminar premixed CH_4/O_2 flame imaged in Fig. 3. The pump beam is vertically polarized and the probe beam is polarized at 45° from the vertical.

intersection of pump and probe beams for linearly and circularly polarized pump beams, respectively. The linearly polarized pump beam is vertical, i.e., polarized normal to the plane of intersection of the pump and probe beams. The images are 50 shot averages. The tip of the burner can be seen at the base of each image. The images have been corrected for the average probe beam profile.

Figure 5 shows the equivalent orthogonal PLPS average image for a linearly polarized pump beam polarized horizontally, i.e., polarized in the plane of intersection of the pump and probe beams. The lack of signal corresponds to the zero signal strength predicted for normal pump–probe beam intersection by Eq. (7) and the $\cot^2(\theta)$ dependence noted by Nyholm *et al.*[2]

The instantaneous images do not differ from the average images, owing to flame stability. Figures 6 and 7 show the image quality of an instantaneous image for a linearly polarized pump beam polarized vertically and for a circularly polarized pump beam, respectively. Maximum instantaneous signal-to-background ratios of 34:1 for a linearly polarized pump beam indicate that a signal-to-background ratio of 1100:1 is possible for an intersection angle of 10° with this polarization configuration. The maximum instantaneous signal-to-background ratios detected for the circularly polarized pump beam were 43:1.

The images do not require elongation in the horizontal direction, as is the case for small intersection angle polarization spectroscopy. The imaged region is ~5–6 mm wide and 4 mm high. The image resolution is 9.5 μm/pixel for both linearly and circularly polarized pump beams. The thickness of the elliptical interaction region was estimated to be 700 μm.

4. Conclusions

We have demonstrated that planar laser polarization spectroscopy is possible for perpendicular pump–probe beam intersection for both linearly and circularly polarized pump beams. Both instantaneous and average orthogonal PLPS images have been pre-

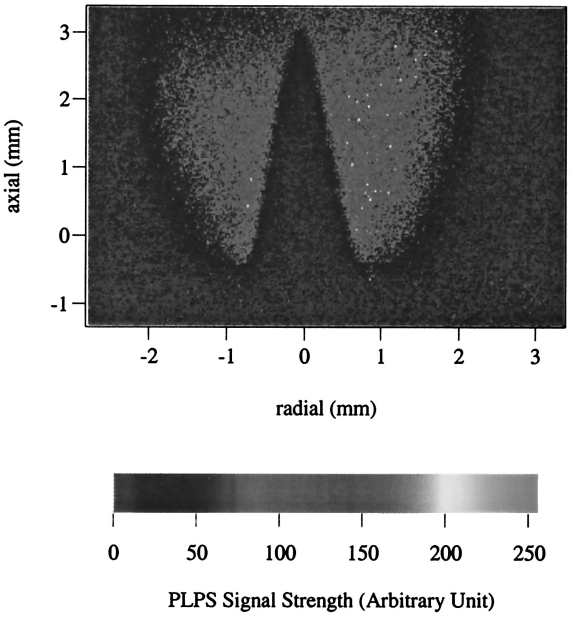

Fig. 7. Instantaneous OH [$A\ ^2\Sigma$–$X\ ^2\Pi$(0–0) $Q_2(8)$ transition] orthogonal PLPS signal for the laminar premixed CH_4/O_2 flame imaged in Fig. 4. The pump beam is circularly polarized and the probe beam is polarized at 45° from the vertical.

sented. For maximum signal strength, the polarization direction of the linearly polarized pump beam should be normal to the plane of intersection of the pump and probe beams and the probe beam polarization should be 45° from that of the pump beam.

The orthogonal PLPS imaging method does not require elongation of the collected image to represent the imaged area, maximizing spatial resolution at the expense of signal strength. However, the small pump–probe beam intersection angle required for significant increases in the signal strength for nonorthogonal PLPS (an increase by a factor of 4 for imaging at 30° pump–probe beam intersection angle and an increase by a factor of 33 for imaging at 10° intersection angle) leads to a significant decrease in the spatial resolution of the technique. Small-angle PLPS is also dependent on the quality of the probe beam profile in the intersection region of pump and probe beams because any imperfection is emphasized by the required stretching of the collected image to represent the elliptical interaction region.

This research was supported by the Australian Research Council.

References

1. C. Wieman and T. W. Hänsch, "Doppler-free laser polarization spectroscopy," Phys. Rev. Lett. **36,** 1170–1173 (1976).
2. K. Nyholm, R. Fritzon, and M. Alden, "Two-dimensional imaging of OH in flames by use of polarization spectroscopy," Opt. Lett. **18,** 1672–1674 (1993).
3. G. Zizak, J. Lanauze, and J. D. Winefordner, "Cross-beam polarization in flames with a pulsed dye laser," Appl. Opt. **25,** 3242–3246 (1986).
4. J. Reppel and Z. T. Alwahabi, "A uniaxial gas model of the geometrical dependence of polarization spectroscopy," J. Phys. D **34,** 2670–2678 (2001).
5. R. E. Teets, F. V. Kowalski, W. T. Hill, N. Carlson, and T. W. Hänsch, SPIE, "Laser Polarisation Spectroscopy," in *Advances in Laser Spectroscopy I*, A. H. Zewail, ed., Proc. SPIE **113,** 80–87 (1977).
6. T. A. Reichardt and R. P. Lucht, "Theoretical calculation of line shapes and saturation effects in polarization spectroscopy," J. Chem. Phys. **109,** 5830–5843 (1998).